Infrared polarisation measurements of surface and buried anti-personnel landmines

Frank Cremer[abc], Wim de Jong[a] and Klamer Schutte[a]

[a]TNO Physics and Electronics Laboratory, P.O. Box 96864, 2509 JG, The Hague, The Netherlands
[b]Pattern Recognition Group, Delft University of Technology, Delft, The Netherlands
[c]Section of Applied Geophysics, Delft University of Technology, Delft, The Netherlands

ABSTRACT

Linear polarisation of Thermal InfraRed (TIR) radiation occurs whenever radiation is reflected or emitted from a smooth surface (such as the top of a landmine) and observed from a grazing angle. The background (soil and vegetation) is generally much rougher and therefore has less pronounced linear polarised radiation. This difference in polarisation can be used to enhanced detection of land mines using TIR cameras.

A measurement setup is constructed for measurement of polarised TIR images. This setup contains a rotating polarisation filter which rotates synchronously with the frame sync of the camera. Either a Long Wave InfraRed (LWIR) or a Mid Wave InfraRed (MWIR) camera can be mounted behind the rotating polarisation filter. The synchronisation allows a sequence of images to be taken with a predefined constant angle of rotation between the images. Out of this image sequence three independent Stokes images are calculated, consisting of the unpolarised part, the vertical/horizontal polarisations and the two diagonal polarisations.

An initial model is developed that describes the polarisation due to reflection of and emission from a smooth surface. This model predicts the linear polarisation for a landmine 'illuminated' by a source that is either hotter or cooler than the surface of them landmine. The measurement setup is used indoors to validate the model. The measurements agree well with the model predictions.

Keywords: infrared polarisation model, measurement setup, measurements, landmine detection

1. INTRODUCTION

One of the sensors that are used to detect landmines is a Thermal InfraRed (TIR) camera. Current cameras are able to detect small temperature differences (as low as 15 mK). Landmines have different heat conductivity and heat capacity compared to natural backgrounds. Temperature differences between a a landmine and the background may develop when the soil is heated or cooled down due to these differences in thermal properties. The TIR radiation from other sources (like the sun) also is reflected on the landmine and the background. Both emission from surfaces and reflection of sources onto these surfaces play a role in the formation of the TIR image.

TIR images of landmines in natural scenes do suffer from clutter, since other (natural) objects like trunks, holes and rocks also may have different thermal properties compared to the background. In the visual spectrum it is well known that unpolarised light reflected from a smooth surface becomes polarised.[4] This is also true for TIR radiation. However, for TIR radiation not only the reflection is polarised, but also the emission is polarised. Since in general the surfaces of landmines are smoother than the surfaces found in a natural background, the presence of significant polarised TIR radiation is an extra indication for landmines (or other non-natural objects). This has been shown in our previous work.[8,14]

In this paper, first an introduction will be given about the background of measuring TIR polarisation. Furthermore, a model of TIR polarisation will be presented along with the model assumptions. For measurements of TIR polarisation, the constructed measurement setup is described. In the next section the indoor measurements are described. These measurements are analysed and compared to the model expectations. Finally, the conclusions are presented, followed by future work on TIR polarisation.

In Figure 1, the relation between the various aspects of TIR polarisation measurements are shown. The camera observes the scene through a polarisation filter. The measured irradiation, consisting of a non-linear polarised and a polarised part, depends on the temperature of the target (mine or background) and the reflection of sources on the target.

Further author information: (Send correspondence to Frank Cremer)
Frank Cremer: E-mail: Cremer@fel.tno.nl Phone: +31 70 374 0795 Fax: +31 70 374 0654
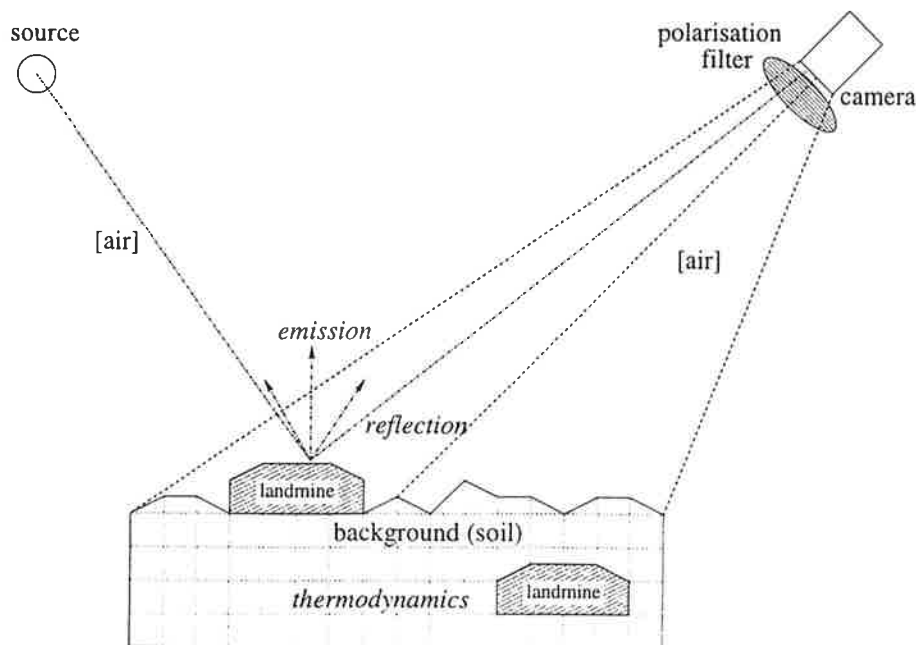
Figure 1. Overview of the various aspects of infrared polarisation. The camera observes the scene through a polarisation filter. The measured irradiation and the polarisation of this irradiation depends on the temperature of the target (landmine or background) and the reflection of sources on the target.

2. POLARISATION MODEL

To describe the polarisation effects a very basic model will be introduced. This model only describes the MWIR polarisation effects on the landmine target illuminated by a single source, see Figure 2. The polarisation of the natural background is not taken into consideration. This model starts from a number of assumptions to simplify the calculations. These assumptions are:

1. The material of the landmine can be described by a single refractive index for the wavelength band used (MWIR) and thus is spectrally independent.

2. The material of the landmine is opaque, meaning that there is no transmission of radiation through the landmine.

3. The surface of the landmine is perfectly specular for reflection and is Lambertian for emission.

4. The landmine is in thermal equilibrium with the surrounding and thus the temperature is constant.

5. The single source, that is reflecting on the landmine, is unpolarised.

6. The spectral sensitivity of the MWIR camera is constant throughout the wavelength band, ranging from 3 to 5 μm.

7. The polarisation filter is ideal for the wavelength band.

8. The transmission through air is 100% and thus there doesn't exist any path radiance.

The source in Figure 2 is assumed to be a black body (meaning that the emission coefficient is 1 over the whole wavelength band) at a fixed temperature T_{bb}. The radiated electro-magnetic wave can be decomposed into two perpendicular components called polarisations. One component vector E_{ip} is in the plane of incidence; this is called parallel polarisation, hence the subscript p. The plane of incidence is the plane which is spanned by the propagation direction of the incidence and the reflected radiation. The other component E_{is} is perpendicular to the plane of incidence and is given the subscript s. These two incidence polarisations are equal in magnitude, as the source is assumed to be unpolarised.
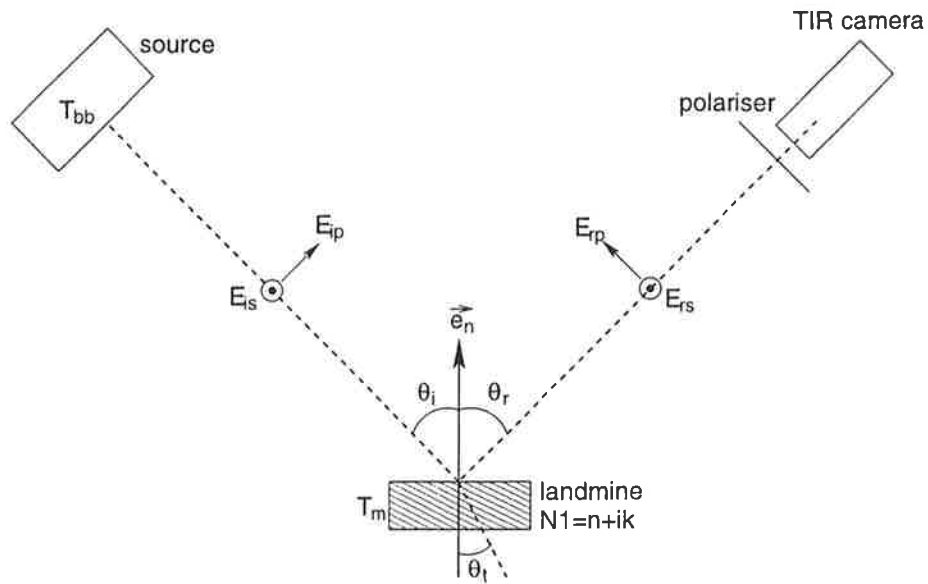
Figure 2. The simplified polarisation model.

The thermal emission of a black body in the MWIR wavelength band as function the temperature T is given by Planck's equation[7]:

$$I_{BB}(T) = \int_{3\mu m}^{5\mu m} \frac{2\pi hc^2}{\lambda^5} \frac{1}{e^{\frac{hc}{\lambda kT}} - 1} \, d\lambda \quad [W/m^2]. \tag{1}$$

with h Planck's constant, k Bolzman's constant and c the speed of light.

The instantaneous electrical field ($E_r p$, $E_r s$) of the TIR radiation cannot be measured by the TIR camera. The frequencies involved are too high to make this measurement possible. Instead, the TIR camera measures the amount of power (per unit area) incident onto the detector, which is called irradiation. For electro-magnetic waves with field strength E, the irradiation is given by:

$$I = \frac{\epsilon_a \, c}{T} \int_0^T E^2 dt \quad [W/m^2], \tag{2}$$

with ϵ_a the dielectric constant of the medium (air) and the integration period T large enough ($T \gg \lambda/c$). The incident irradiation on the landmine can be described by two irradiation terms I_{ip} and I_{is}, that are related to E_{ip} and E_{is} respectively. These two incident irradiation terms are equal in magnitude and the sum of these terms is equal to the black body irradiation as given in Equation 1:

$$I_{ip}(T_{bb}) = I_{is}(T_{bb}) = \frac{1}{2} I_{BB}(T_{bb}) \tag{3}$$

The surface of the landmine in Figure 2 is assumed to be specular for reflection. The angle of incidence θ_i is equal to the angle of reflection θ_r. To determine the reflection coefficients, it is necessary to define the angle of transmission θ_t, even though the transmission is assumed to be zero. The relationship between the angle of incidence θ_i and the angle of transmission θ_t is given by Snell's law[4]:

$$N_0 \sin(\theta_i) = N_1 \sin(\theta_t), \tag{4}$$

with N_0 the refractive index of the air and $N_1 = n + i\,k$ the refractive index of the landmine (in complex notation). The refractive index of the air is assumed to be 1, so $N_0 = 1$. The refractive index of the landmine is unknown, but will be calculated in Section 5.

Part of the irradiation originating from the source is reflected by the surface. The amount that will be reflected is given by the reflection coefficients, which differ for the two polarisation orientations. The reflection coefficients, in terms of irradiation.

are given by[4]:

$$\rho_p(\theta_i) \;=\; \frac{I_{rp}}{I_{ip}} = \left(\frac{E_{rp}}{E_{ip}}\right)^2 \;=\; \left(\frac{\tan(\theta_i - \theta_t)}{\tan(\theta_i + \theta_t)}\right)^2 \tag{5}$$

$$\rho_s(\theta_i) \;=\; \frac{I_{rs}}{I_{is}} = \left(\frac{E_{rs}}{E_{is}}\right)^2 \;=\; \left(\frac{-\sin(\theta_i - \theta_t)}{\sin(\theta_i + \theta_t)}\right)^2 \tag{6}$$

The remaining of the irradiation from the source is either transmitted through or absorbed by the landmine. The transmission through the landmine is assumed to be zero. The emission coefficient ϵ of irradiation from the landmine is equal to the absorption coefficient, under the assumption that the landmine is in thermal equilibrium with the environment. So the emission coefficients for both polarisation orientations are given by:

$$\epsilon_p(\theta_i) \;=\; 1 - \rho_p(\theta_i) \tag{7}$$

$$\epsilon_s(\theta_i) \;=\; 1 - \rho_s(\theta_i). \tag{8}$$

The irradiation from the landmine consists of the reflected irradiation from the source and the emitted irradiation due to the temperature T_m of the surface of the landmine:

$$I_p(T_m, T_{bb}, \theta_i) \;=\; \tfrac{1}{2} I_{BB}(T_m)\, \epsilon_p(\theta_i) + \tfrac{1}{2} I_{BB}(T_{bb})\, \rho_p(\theta_i) = \;\; \frac{1}{2} I_{BB}(T_m) + \frac{1}{2}\rho_p(\theta_i)\left[I_{BB}(T_{bb}) - I_{BB}(T_m)\right]. \tag{9}$$

$$I_s(T_m, T_{bb}, \theta_i) \;=\; \tfrac{1}{2} I_{BB}(T_m)\, \epsilon_s(\theta_i) + \tfrac{1}{2} I_{BB}(T_{bb})\, \rho_s(\theta_i) = \;\; \frac{1}{2} I_{BB}(T_m) + \frac{1}{2}\rho_s(\theta_i)\left[I_{BB}(T_{bb}) - I_{BB}(T_m)\right]. \tag{10}$$

This irradiation passes through an (assumed to be) ideal polariser and subsequently onto the detector array of the camera. The detector of the camera returns a value linear to the incoming irradiation. This value depends on the orientation of the filter. For a given angle φ between the principal axis of the polarisation filter and the horizontal axis, the irradiation I_c as measured by one detector element of the camera is given by:

$$I_c(\varphi) = \frac{1}{2}\frac{\Omega_c}{\pi}\left[I + Q\cos(2\varphi) + U\sin(2\varphi)\right], \tag{11}$$

where $\varphi = 0$ represents the situation that horizontal polarised radiation passes through the linear polariser unattenuated. The solid angle Ω_c is the instantaneous field of view of the detector element. For the remainder of this section this solid angle Ω_c is assume to be π. The parameters I, Q and U are three of the four Stokes parameters. The fourth parameter V defines the circular polarisation and is not considered in the model and cannot be measured by a linear polarisation filter.

The Stokes parameters relate to the total intensity as given in Equation 10 as follows:

$$I_c(90°) \;=\; \tfrac{1}{2} I - \tfrac{1}{2} Q = \;\; I_p(T_m, T_{bb}, \theta_i), \tag{12}$$

$$I_c(0°) \;=\; \tfrac{1}{2} I + \tfrac{1}{2} Q = \;\; I_s(T_m, T_{bb}, \theta_i), \tag{13}$$

this only defines two Stokes parameters (I and Q). The third parameter U (diagonal polarisation) must be 0, since in this situation only horizontal (perpendicular) $T_{bb} > T_m$ or vertical (parallel) $T_m > T_{bb}$ polarisation can exist.

Often a different representation is used for the polarisation:

$$LP \;=\; \sqrt{Q^2 + U^2}, \tag{14}$$

$$\omega \;=\; \frac{1}{2}\arctan(U/Q), \tag{15}$$

with LP the amount of linear polarisation and ω the angle of polarisation. In this specific situation the angle ω is either 0° ($T_{bb} > T_m$) or 90° ($T_m > T_{bb}$). The linear polarisation is in this specific situation equal to the absolute value of Q and thus is given by:

$$
\begin{aligned}
LP(T_m, T_{bb}, \theta_i) \;&=\; \mathrm{abs}[I_s(T_m, T_{bb}, \theta_i) - I_p(T_m, T_{bb}, \theta_i)]\\
&=\; \frac{1}{2}\mathrm{abs}\left[(\rho_s(\theta_i) - \rho_p(\theta_i))\,(I_{BB}(T_{bb}) - I_{BB}(T_m))\right].
\end{aligned}
\tag{16}
$$

In Figure 3 the linear polarisation is plotted for a range of incidence angles θ_i and differences in black body temperature ΔT around 291.6 K). For the refractive index of the landmine surface the value $1.1 + 0.30i$ is chosen.
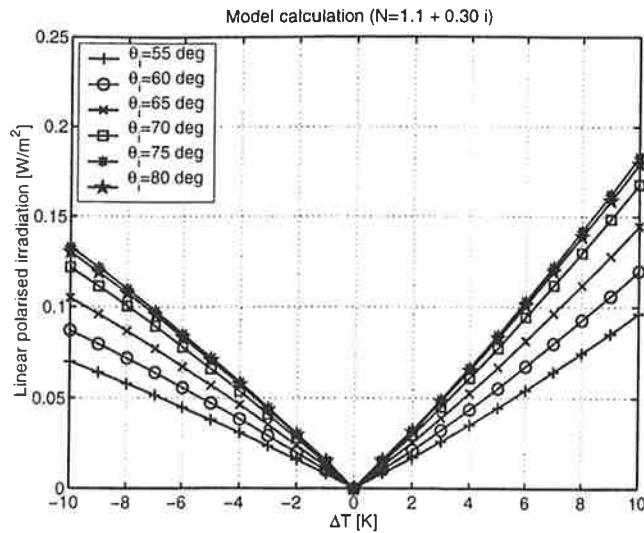
Figure 3. The linear polarised irradiation as calculated by the model for temperature differences ΔT between the landmine and the heat source (the landmine had a temperature of 18.43 degrees). The angle of incidence θ_i is varied between 50 and 80 degrees.

3. MEASUREMENT SETUP

3.1. Related work

Generally there are two different approaches used for the measurement of the infrared polarisation. Either time division or spatial division is used. However, at least two other approaches claim not to suffer from this division; they are discussed at the end of this section.

With time division, different polarisation images are measured one after each other. This is usually performed by mounting a polarisation filter in front of the camera and taking a sequence of images with different polarisation. Instead of rotating the polarisation filter, it is also possible to rotate a quarter-wave plate. This approach of either rotating a polariser or a quarter-wave plate is used by the majority of the authors.

Alternatively, the different polarisations are measured simultaneously at the cost of reduced spatial resolution. For example, every 4 adjacent pixels of a focal plane array (FPA) are grouped. In front of each of these 4 pixels a different polarisation filter is mounted, each with a different orientation. This approach is followed by two parties. First there is Nichols Research in cooperation with DERA (UK)[1] and the University of Alabama.[11] Secondly, there is Physics Innovations[2] in cooperation with Lockheed Martin.[12] Because of the larger development costs, this approach is less common. However, due to the fact that a full set of four Stokes images can be acquired in a single frame, this approach has advantages for applications in fast changing environments.

There are at least two other approaches that claim not to suffer from either time or spatial division. The first one is a hyper spectral imager as made by Aerodyne.[6] The other is developed by FOI (Swedish patent FOA-R-99-01090-408-SE) and is a construction of a stack of detector elements, where each element only detects one polarisation direction and passes the others.

3.2. Construction

Our approach for the measurement setup is the use of time division and a rotating polarisation filter. An overview of this setup is given in Figure 4(a). The setup consists of a wire-grid polariser, a motor to rotate the polariser and controller electronics. In this setup different infrared cameras can be mounted. The polarisation filter has a large spectral range and thus can be used for either Long Wave InfraRed (LWIR) or Mid Wave InfraRed (MWIR) cameras.

The controller electronics has the task to synchronise the rotation of the polarisation filter with the frame sync of the camera. In Figure 4(b), the motor controller is shown in more detail. For each rotation of the filter between 6 and 60 frame syncs of the camera occur, depending on how the multiplier is set. For the motor speed control there are two options: either the angle read out is divided by a number or the frame sync is multiplied. If the angle read out is divided, then the frequencies that the Phase

(a)

(b)
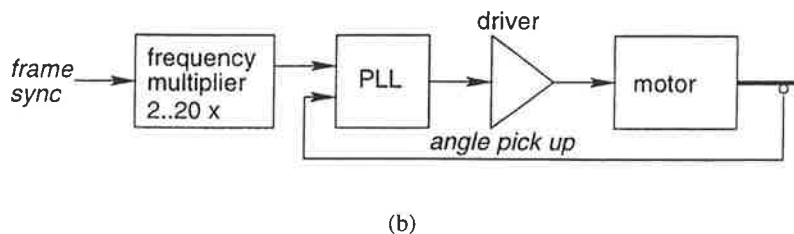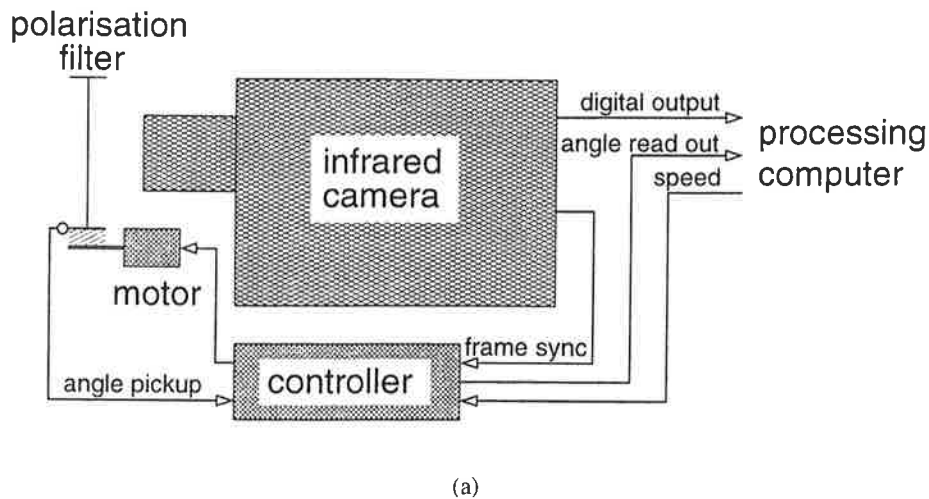
Figure 4. a) Infrared polarisation setup, consisting of a wire-grid polariser, a motor, an infrared camera and custom-made controller electronics. b) The motor controller multiplies the frame sync by a number as given by the processing computer. This is input to the Phase Locked Loop (PLL), which drives the motor so that the angle pick up has the same frequency as the multiplied frame sync. The angle pick up gives a pulse for every 3 degrees of rotation.

Lock Loop (PLL) tries to match is the same as the frame sync frequency. Due to these low frequencies the controller dynamics have a tendency to become unstable.

We have chosen for multiplying the frame sync, instead of dividing the angle read out. Because of this multiplication the PLL works at a higher frequency and can make faster speed corrections. With this multiplication the PLL is in lock even for the lowest rotation speed of 1 rotation per second. The angle read out is also counted (and reset for each rotation) so that the angle can be recorded for each frame sync.

One problem of this setup is that the polarisation filter is reflecting radiation from the camera housing, the lens and through the lens the cooled detector array. This image seems to be out of focus. So, instead of just acquiring the image of the scene, the reflected image is added to it. This effect is called narcism. There are two ways of correcting this effect. The first one is to tilt the polariser so that it does not look at the camera, but at a uniform source. For a small Field Of View (FOV) this tilting seems possible. However, when observing mines at relative close distance (a few meters), a wide FOV lens is necessary. The filter has to be tilted much more (more than a couple of degrees). It is expected that this tilting may give rise to problems (the transmission through the filter may change) and seems therefore not feasible.

The second approach for correcting narcism is to measure this reflected image of the filter. This measured reflection is subsequently subtracted from the acquired scene image. For different angles of the polarisation filter, the reflected image may be different. To compensate for those differences, the reflected image is measured for all the angles that are used to measure the scene. When subtracting two independent images such as the scene and the reflection image, the noise will be doubled. To reduce this noise, 30 narcism images are acquired for each angle and these images are averaged.
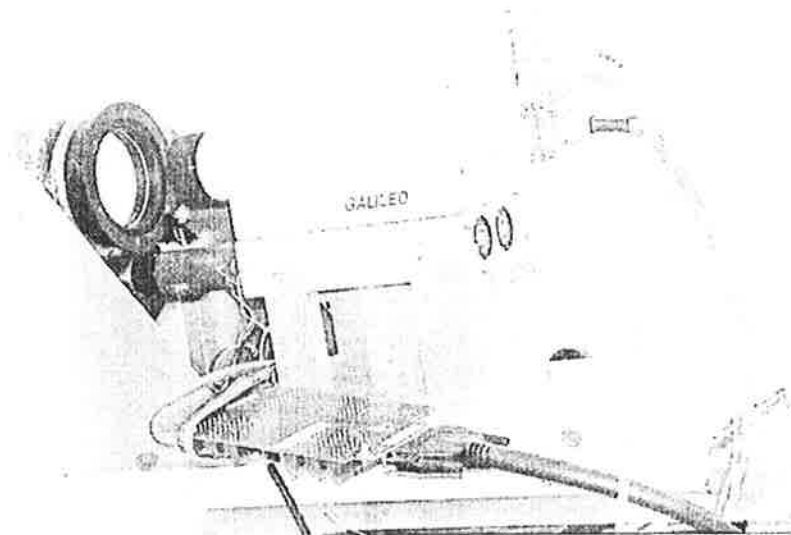
Figure 5. Photo of the infrared polarisation setup

4. MEASUREMENTS

4.1. System calibration

The camera measures the integrated irradiation over some integration period (usually in the magnitude of 1 ms). This value is digitised with a resolution of 12 bits. The actual value depends on the instantaneous field of view (as given by the solid angle Ω_c in Equation 11), the aperture (lens diameter), the efficiency of the detector as well as the conversion offset.

When all these parameters are known, the measured bit value can be converted to irradiation in W/m^2. However, since all of these parameters are not known (exactly), an other approach is to perform a calibration measurement. The camera with the polariser is viewing a temperature controlled hot/cold black body source. For five temperatures around 291.6 K, measurements are taken. The average irradiation (the Stokes parameter I) in terms of bit value I_{bit} is calculated over a full rotation of the polariser, see Section 5.

The irradiation in W/m^2 for a black body of these temperatures is given by $I_{BB}(T)$ in Equation 1. The camera returns an average value $I_{bit}(T)$ over the part of the image containing the black body. The irradiation $\tilde{I}_{BB}(T)$ is assumed to be linear with this bit value:

$$\tilde{I}_{BB}(T) = a\, I_{bit}(T) + b \tag{17}$$

The parameters a and b are calculated by minimisation of the difference between measured irradiation $\tilde{I}_{BB}(T)$ and the black body radiation $I_{BB}(T)$. With a Nelder-Mead minimalisation[10] of the sum square error, the parameters $a = 0.00287$ W/m^2 and $b = 4.32$ W/m^2 are obtained.

In Figure 6 the measured irradiation $\tilde{I}_{BB}$ as function of the temperature around 291.6 K is shown after conversion. The difference between this fit and the calculated value I_{BB} is less than $4 \cdot 10^{-3}$ W/m^2. This small difference shows that the assumption of linearity is correct.

The calibration of the polarised irradiation can be performed using a second polariser.[5] Since this polariser is currently not available and other calibration methods are not so easy to set up, this calibration has not been performed. Alternatively, the fabrication specification may possibly be used instead of calibration. This has not been included in the model, so for the remainder of the paper it is assumed that the polariser is ideal for the MWIR wavelength band.

4.2. Indoor landmine measurements

A measurement setup, analog to the model as shown in Figure 2, is used to determine the polarisation effects of the hot/cold black body source reflecting on a landmine. The landmine that is chosen for this experiment is a dummy PMN,[9] see Figure 7.

This landmine has a flat rubber top. This (non-structured) flat top makes it easier to carry out the measurements, because the whole surface can be used. Measurements are taken for six different incident angles between 55 and 80 degrees with steps
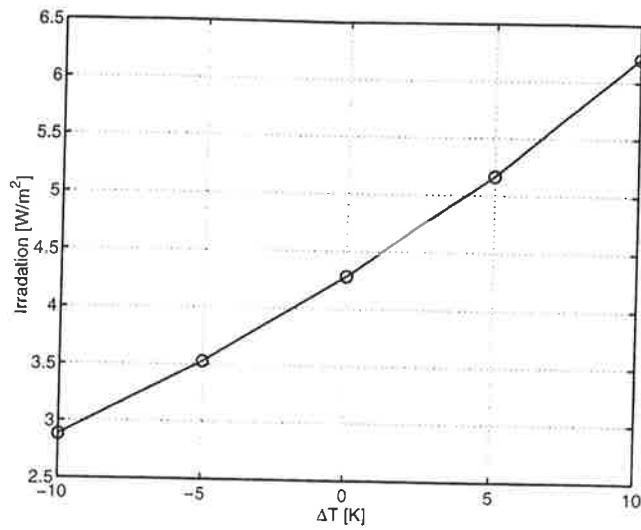
Figure 6. The irradiation as measured by the system (camera and polariser) for a temperature range around 291.6 K. The difference between the calculated (Planck) and measured irradiation is less than $4 \cdot 10^{-3}$ W/m^2.
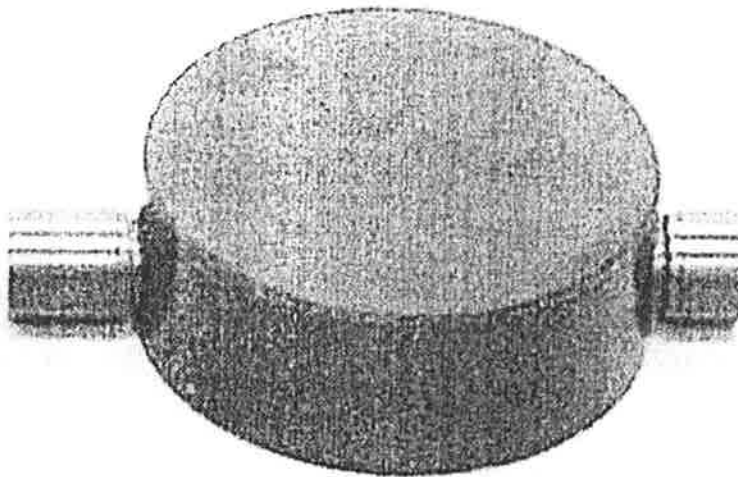
Figure 7. The dummy PMN landmine that was used for the indoor measurements.

(a) $\bar{I}$ (b) $\bar{LP}$ (c) $\bar{\omega}$
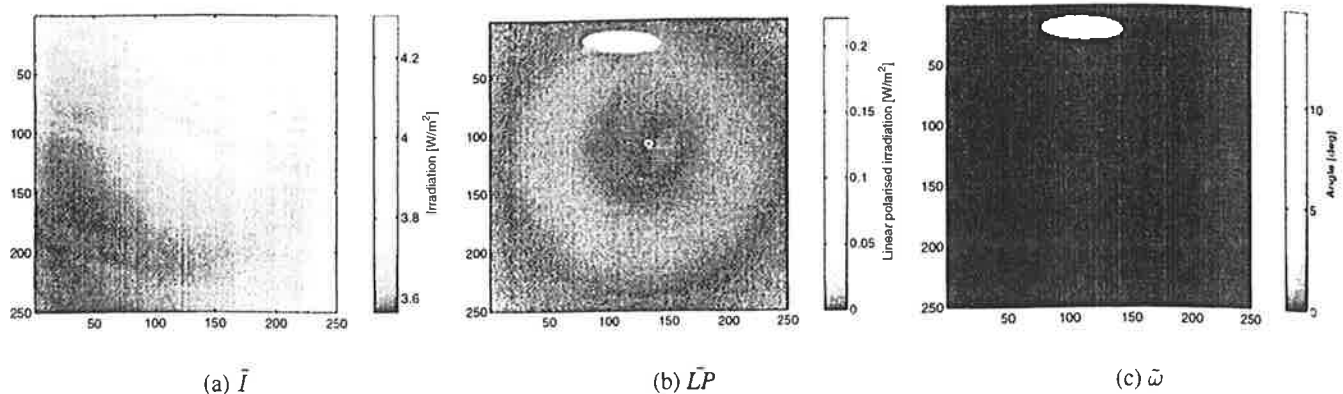
Figure 8. One set of images for $\Delta T = 10\ K$ and $\theta_i = 70$ degree. The irradiation $\bar{I}$ is given in a). The linear polarised irradiation $\bar{LP}$ is given in b) and the angle of polarisation $\bar{\omega}$ for pixels with sufficient linear polarised irradiation is given in c); the remaining of the pixels are set to an angle of 0 degree.

of 5 degrees. The distance between the landmine and the camera was 135 cm. The ambient temperature of the room and thus of the mine was 291.6 K.

The hot/cold source is varied between -10 K and +10 K around ambient temperature. A sequence of images is taken for every 1 K change in temperature. Each sequence consists of 60 images, with the polariser rotated for 6 degrees between two images. The acquisition time is 1 s for each sequence.

5. ANALYSIS

The irradiation as measured by the camera behind the polariser is given in Equation 11. This irradiation is measured for a full rotation of the filter. The Stokes-Müller polarisation parameters $\tilde{I}$, $\tilde{Q}$ and $\tilde{U}$ are estimated by:

$$\tilde{I} = \frac{2}{N} \sum_{i=1}^{N} I_c(\varphi_j)$$

$$\tilde{Q} = \frac{4}{N} \sum_{i=1}^{N} I_c(\varphi_j) \cos(2\varphi_j)$$

$$\tilde{U} = \frac{4}{N} \sum_{i=1}^{N} I_c(\varphi_j) \sin(2\varphi_j), \tag{18}$$

with $N = 60$ the number of frames, j the frame number and $\varphi_j = \frac{2\pi j}{N}$ the angle of the linear polariser for frame i. The angle of the polariser has not been calibrated, so instead of directly using the Stokes parameter Q, the estimated linear polarised irradiation $\tilde{LP}$ is used, using Equation 14.

In Figure 8, the irradiation $\tilde{I}$, the linear polarised irradiation $\tilde{LP}$ and the polarisation angle $\tilde{\omega}$ are shown for the angle of incidence $\theta_i = 70°$ with the source set at 10 K above the ambient temperature (291.6 K).

The irradiation $\tilde{I}$ in Figure 8 clearly shows the top of the landmine. The side and the background is barely visible, because they have a much lower irradiation. The dot in the centre of the image is a residue of the narcism correction. The mine is placed in the top of the field of view to prevent problems with this residue. The linear polarised irradiation of the top of the landmine is much higher then the side and the background. The angle is only shown for pixel that have large enough linear polarised irradiation (more than 0.045 W/m²), which is effectively only the top of the landmine. The angle is 15 degree, but according to the model this should be 0 degree. This difference shows that there is an offset in the uncalibrated angle measurements of around 15 degree.

These measurements are carried out for six different angles and 21 different temperatures. This gives a total of 126 sequences. For every sequence the surface of the mine is selected and the average linear polarised irradiation $\tilde{LP}$ and the average polarisation angle $\tilde{\omega}$ is calculated. The results of these calculations are shown in Figure 9.

(a) Linear polarised irradiation
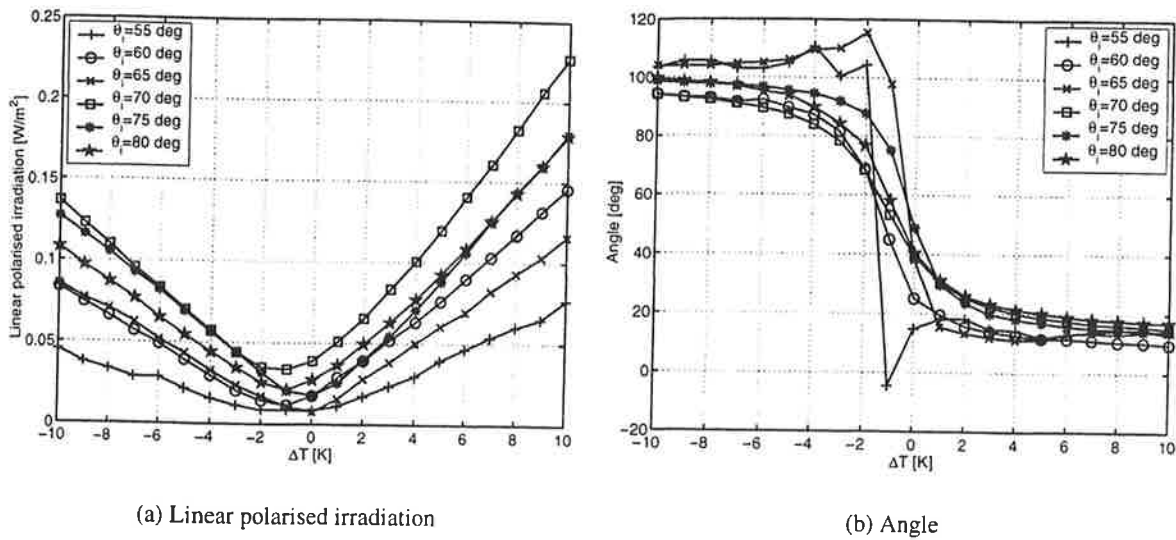
(b) Angle

Figure 9. The linear polarised irradiation and angle as function of the temperature difference and the reflection angle

The minimum of the linear polarised irradiation seems to have shifted to $\Delta T = -1$ K. This shift can also be seen in the angle plot; all curves cross the θ_i=45 degree line between $\Delta T = -2$ K and $\Delta T = 0$ K. An explanation of this might be that the ambient temperature is measured at the side of the source. It cannot be excluded that there is a small temperature difference between this measured temperature and the temperature of the landmine.

In the angle plot, it is expected that there is an abrupt change of angle from 90 degrees to 0 degrees at $\Delta T = 0$ K. However, the plot shows a gradual change of angle between $\Delta T = -6$ K and $\Delta T = 4$ K. Theoretically this cannot be caused by the surface of the landmine, due to the geometry only two orientations are possible (0 and 90 degree). This gradual change probably is caused by contribution of other radiation sources in the indoor test facility. All sources in the plane source-landmine-camera will give either 0 or 90 degree for the angle of polarisation. This implies that there must be other sources outside the plane source-landmine-camera that are reflected on the surface of the landmine. Since these sources are outside of this plane, there also must be diffuse reflection on the surface and thus assumption 3 of the model is not valid.

The difference between Equation 11 using the estimates of the Stokes parameters ($\tilde{I}, \tilde{U}$ and $\tilde{Q}$) and the actual measured irradiation is assumed to be caused by noise.[8] The standard deviation of this noise is 0.015 W/m² for the image set with $\theta_i = 70$ degree and $\Delta T = 10$ K. Since these Stokes parameters are estimated over 60 images, the standard deviation of the noise on $\tilde{I}$ is 0.0019 W/m² ($\sqrt{N}$ times lower than on each pixel) and on $\tilde{Q}$ and $\tilde{U}$ the standard deviation is 0.0027 W/m² ($\sqrt{N/2}$ times lower than on each pixel. This noise on $\tilde{Q}$ and $\tilde{U}$ results into a bias (offset) on $\tilde{LP}$ of 0.0034 W/m² and a standard deviation of 0.0018 W/m². This bias and standard deviation on $\tilde{LP}$ are calculated in a numerical simulation with $\tilde{Q}$ and $\tilde{U}$ normal distributed with zero means and the calculated standard deviation.

Another remarkable fact of Figure 9(a) is that the minimum of the linear polarised irradiation is not zero. Only a small part (0.0034 W/m²) of this is explained by the noise of the camera. The remainder indicates the existence of forementioned sources that also cause a gradual change in angle.

What can be learned of this is that shielding the scene of heat sources is important. Shielding can be performed with materials that have the same temperature as the landmine. Furthermore the temperature of the landmine should also be measured.

Using these measurements, it is possible to estimate the average refractive index over the wavelength band. Since the errors in linear polarised irradiation for low temperature differences is expected to be larger than for higher temperature differences, only the extremes at $\Delta T = -10$ K and $\Delta T = 10$ K are used. The sum square error between the predicted linear polarised irradiation $LP(T)$ and the measured linear polarised irradiation $\tilde{LP}(T)$ is minimised using Nelder-Mead minimalisation over the refractive index. In Figure 10, these measurements and the model expectations for the calculated refractive index is shown.

The measurements in Figure 10 do show large differences between adjacent measurements. This likely to be a result of the fact that these measurements were taken during two different sessions. In one session the angles 55, 65 and 75 degrees are measured and in the other session the angles 60, 70 and 80 degrees are measured. There might have been a change in temperature
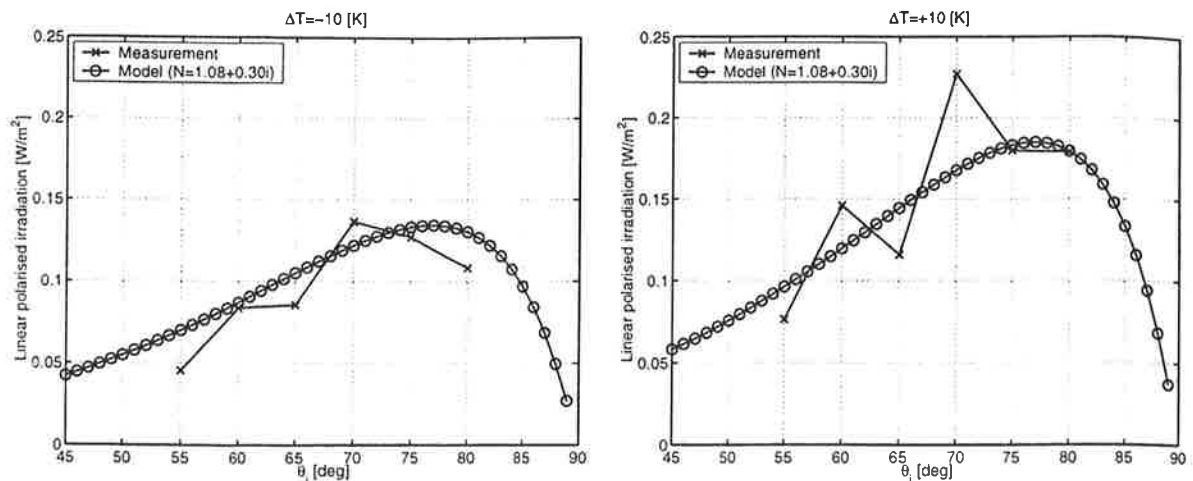
Figure 10. The refractive index of the model is chosen so that the error between the expected (model) and measured linear polarised irradation is minimal. This fit is performed simultaneously for $\Delta T = -10$ K and $\Delta T = 10$ K.

and there may be an offset difference in the angles between the series. Considering the large variation in the measurement value the optimal fit of the refractive index is reasonable close. However, it is expected that the estimated refractive index is not determined very accurately. The irradiation in Figure 10 should be corrected for the bias in $\bar{LP}$, however this bias is quite low compared to the variation in the measurements, so the estimated refractive index will not change significantly.

Note that the maximum linear polarised irradiation as shown by the model in Figure 10 is not found for the Brewster angle $\arctan(\frac{N_1}{N_0}) = 49$ degree. For the Brewster angle the reflected irradiation is fully polarised, however due to emission of the surface the angle of maximum linear polarised irradiation is shifted towards a more grazing angle.

6. CONCLUSIONS AND DISCUSSION

In this paper, a simple model of infrared polarisation is presented. This model predicts the irradiation due to reflection of and emission from a perfectly smooth surface under a number of assumptions. This model shows that if the source illuminating the target has a different temperature than the target, the irradiation is partly polarised.

Also in this paper we present an experimental measurement setup for measurements of polarisation irradiation in the MWIR and LWIR wavelength bands. This setup consists of a rotating polariser and this principle is used by many others. The rotation of the polariser is synchronous with the frame sync. For narcism (reflection of the camera housing on the polariser) is corrected by measuring this reflection for each angle over 30 frames and subtracting it from the scene measurements.

Using this setup, indoor measurements are performed on a PMN landmine. For six different incidence angles and 21 temperatures, the polarised irradiation is measured. These measurements show quite some variations, perhaps because they were measured in two different sessions. A model fit is made and results into an estimated average refraction index (for MWIR) of $1.08 + 0.30 \cdot i$ for the top of the PMN landmine.

The existence of noise on the estimated Stokes parameters results into a bias (offset) of the estimated linear polarised irradiation. This bias is small compared to the variations within the measurement sessions. The consequence for the estimation of the refractive index is low.

7. FUTURE WORK

It is necessary to validate the proposed model using more accurate measurements. To improve the accuracy we propose the following:

- Do all measurement in one session and improve on the measurement of the angle of incidence.

- Try to shield of all possible heat sources, so that only the landmine and the black body influence the scene.

- During the time of measurements, more measurements of temperatures should be made: The temperature of the landmine and the environment should be monitored at all times.

- Include a calibration of the polariser. There seems to be an offset error in the orientation of the filter. The characteristics of the polariser also should be determined (measured or based on the specifications).

- Apply the fit of the model, using the Stokes parameter Q instead of the linear polarised irradiation LP.

- More possible sources of error should be determined and quantified.

Besides improving on the measurement accuracy, a comparison between MWIR and LWIR should be made. Measurements of different landmines should be done. With the results of these measurements, an estimate can be made about what is the most optimal measurement setup (viewing angle, weather conditions) to detect landmines in a realistic outdoor environment.

Finally, it is our intention to evaluate the application of the TIR polarisation setup as a replacement for the TIR camera in a sensor-fusion system. The sensor-fusion system, consisting of a Ground Penetrating Radar (GPR) a Metal Detector (MD) and a TIR camera, has shown improvement in detection performance over a single sensor system.[3,13]

REFERENCES

1. H. Barnes, M. Jones, and P. Bishop. Infrared polarimetric camera system development. In A. C. Dubey and J. F. Harvey, editors, *Proc. SPIE Vol. 3710, Detection and Remediation Technologies for Mines and Minelike Targets IV*, pages 189–196, Orlando (FL), USA, Apr. 1999.

2. C. S. L. Chun, D. L. Fleming, W. A. Harvey, and E. J. Torok. Polarization-sensitive thermal imaging sensors for target discrimintation. In W. R. Watkins and D. Clement, editors, *Proc. SPIE Vol. 3375, Targets and Backgrounds: Characterization and Representation IV*, pages 326–336, Orlando (FL), USA, Apr. 1998.

3. F. Cremer, J. G. M. Schavemaker, E. den Breejen, and K. Schutte. Towards an operational sensor fusion system for anti-personnel landmine detection. In A. C. Dubey, J. F. Harvey, J. T. Broach, and R. E. Dugan, editors, *Proc. SPIE Vol. 4038, Detection and Remediation Technologies for Mines and Minelike Targets V*, pages 792–803, Orlando (FL), USA, Apr. 2000.

4. E. Hecht. *Optics*. Addison-Wesley publishing company, Reading (MA), USA, second edition, 1987.

5. J. D. Howe, M. A. Miller, R. V. Blumer, T. E. Petty, M. A. Stevens, D. M. Teale, and M. H. Smith. Polarization sensing for target acquisition and mine detetection. In D. H. Goldstein, D. B. Chenault, W. G. Egan, and M. J. Duggin, editors, *Proc. SPIE Vol. 4133, Polarization Analysis, Measurement, and Remote Sensing III*, San Diego (CA), USA, July 2000.

6. F. J. Iannarilli, Jr, J. A. Shaw, S. H. Jones, and H. E. Scott. Snapshot LWIR hyperspectral polarimetric imager for ocean surface sensing. In D. H. Goldstein, D. B. Chenault, W. G. Egan, and M. J. Duggin, editors, *Proc. SPIE Vol. 4133, Polarization Analysis, Measurement, and Remote Sensing III*, San Diego (CA), USA, July 2000.

7. P. A. Jacobs. *Thermal infrared characterization of ground targets and backgrounds*. SPIE Optical Engineering Press, Bellingham (WA), USA, 1996.

8. W. de Jong, F. Cremer, K. Schutte, and J. Storm. Usage of polarisation features of landmines for improved automatic detection. In A. C. Dubey, J. F. Harvey, J. T. Broach, and R. E. Dugan, editors, *Proc. SPIE Vol. 4038, Detection and Remediation Technologies for Mines and Minelike Targets V*, pages 241–252, Orlando (FL), USA, Apr. 2000.

9. C. King, editor. *Jane's mines and mine clearance*, volume 98-99. Jane's Information Group, Surrey, UK, 3rd edition, 1998.

10. J. C. Lagarias, J. A. Reeds, M. H. Wright, and P. E. Wright. Convergence properties of the nelder-mead simplex method in low dimensions. *SIAM Journal of Optimization*, 9(1):112–147, 1998.

11. G. P. Nordin, J. T. Meier, P. C. Deguzman, and M. W. Jones. Micropolarizer array for infrared imaging polarimetry. *Journal of Optical Society of America*, 16(5):1168–1174, May 1999.

12. F. A. Sadjadi and C. S. Chun. Application of a passive polarimetric infrared sensor in improved detection and classification of targets. *International Journal of Infrared and Millimeter Waves*, 19(11):1541–1559, 1998.

13. J. G. M. Schavemaker, E. den Breejen, F. Cremer, K. Schutte, and K. W. Benoist. Depth fusion for anti-personnel landmine detection. In A. C. Dubey, J. F. Harvey, J. T. Broach, and V. George, editors, *Proc. SPIE Vol. 4394, Detection and Remediation Technologies for Mines and Minelike Targets VI*, Orlando (FL), USA, Apr. 2001.

14. J. Storm and T. Geisler. Trip wire detection using polarimetric IR. In A. C. Dubey, J. F. Harvey, J. T. Broach, and R. E. Dugan, editors, *Proc. SPIE Vol. 4038, Detection and Remediation Technologies for Mines and Minelike Targets V*, pages 253–260, Orlando (FL), USA, Apr. 2000.